



Hydrological investigation of climate change impact on water balance components in the agricultural terraced watersheds of Yemeni highland

Ali H. AL-Falahi¹ · Naeem Saddique² · Uwe Spank¹ · Thomas Pluntke¹ · Solomon H. Gebrechorkos^{3,4} · Matthias Mauder¹ · Christian Bernhofer¹

Received: 10 September 2023 / Accepted: 26 February 2024
© The Author(s) 2024

Abstract

Hydrological models serve as valuable instruments for assessing the impact of climate change on water resources and agriculture as well as for developing adaptation measures. In Yemen, climate change and variability are imposing a significant impact on the most important sectors such as agriculture and economy. The current study evaluates the influence of future climate on hydrology and water balance components in Yemen's highlands using a semi-distributed physical-based hydrologic model Soil Water Assessment Tool (SWAT) and employing high-resolution climate projections. The SWAT was calibrated and verified using observed streamflow data from 1982 to 2000 in three large catchments. Ground data from 24 stations and statistically downscaled future climate data for the period 2010–2100 under RCP2.6 and RCP8.5 are used. SWAT performance was assessed using multiple statistical methods, which revealed the commendable performance of SWAT during the calibration (average NSE = 0.80) and validation (NSE = 0.72) periods. The outcome indicates an increase in future seasonal and annual rainfall, maximum temperature, and minimum temperature in the 2020s and the 2080s under both RCP2.6 and RCP8.5 scenarios. This projected increase in the rainfall and the local temperature will result in increased averages of surface runoff, evapotranspiration, soil water, and groundwater recharge in the representative three catchments up to 6.5%, 21.1%, 7.6%, and 6.4%, respectively. Although, the projected increase in the water balance components will benefit the agriculture and water sector, specific adaptation measures will be crucial to mitigate potential flood impacts arising from the increased precipitations as well as to minimize the consequences of the increased temperature. Likewise, demand for supplementary irrigation is expected to increase to offset the higher evapotranspiration rates in the future.

1 Introduction

Water management is a paramount concern in arid and semi-arid regions as it substantially affects local livelihoods, land productivity, and social welfare. For millennia,

residents of these areas have developed various water-harvesting mechanisms to cope with water scarcity such as capturing surface runoff from sparsely vegetated mountain slopes and diverting occasional wadi flow to irrigate croplands (Magombeyi et al. 2018; Pani et al. 2021). The highland reign of Yemen offers a prime example of how scarce water resources are managed in the semi-drylands. The region is located at the northwest of Yemen between longitude 43 and 45° East and 14 and 16° North (Fig. 1). The region occupies an area of 39,400 Km² and is characterized by high elevation (3,660 m), complex topography, and a large population density. Compared to the other zones of Yemen, the region enjoys a moderate climate throughout the year with an average temperature of about 24 °C. The rainy season extends from March–May and from July–September with average annual rainfall ranging from 300 in the east to 400 mm in western districts. Rain is influenced by two mechanisms; The Red Sea Convergence

✉ Ali H. AL-Falahi
ali.al-falahi@tu-dresden.de

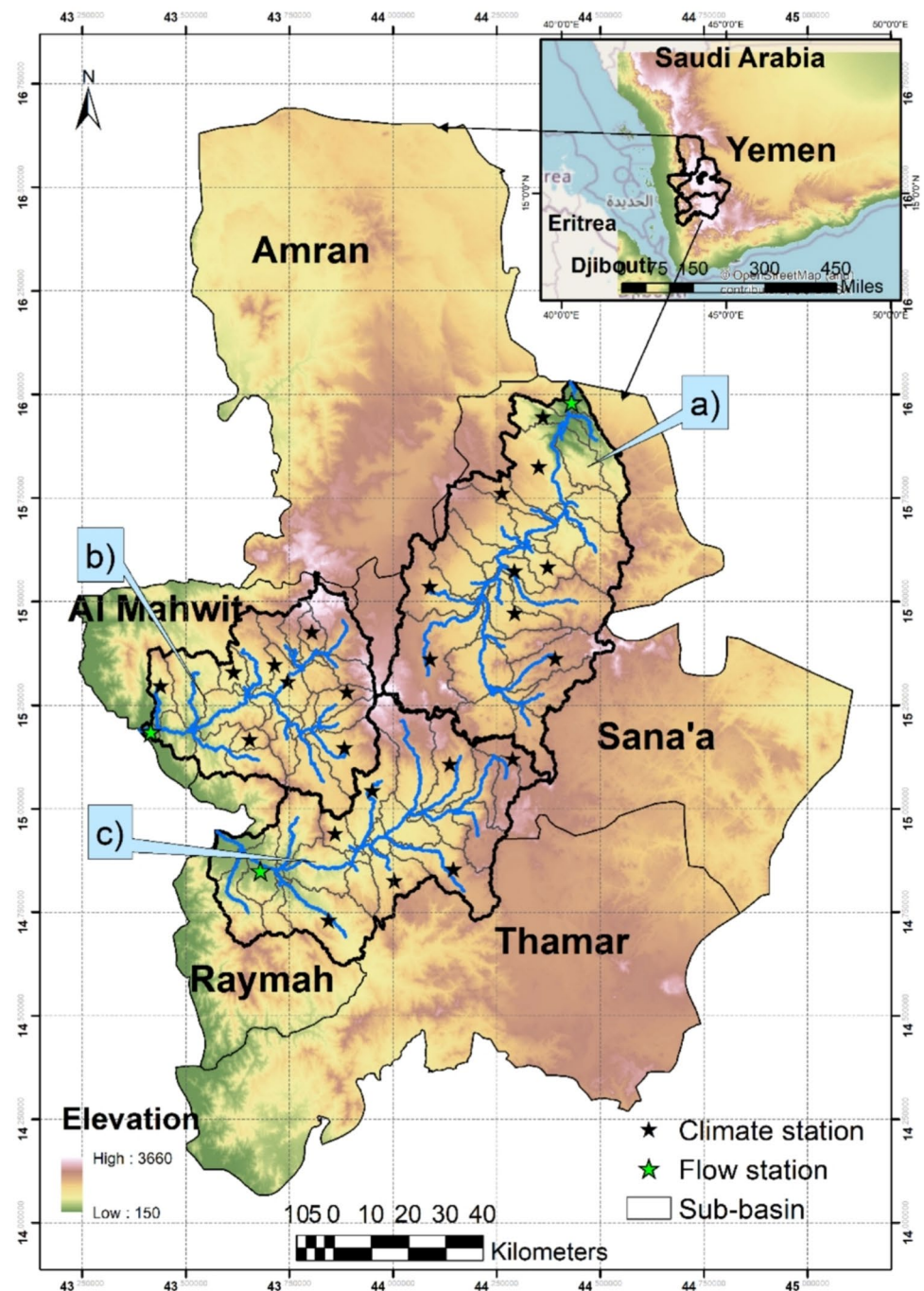
¹ Institut Für Hydrologie Und Meteorologie, Technische Universität Dresden, Piennner Str. 23, 01737 Tharandt, Germany

² Department of Irrigation and Drainage, University of Agriculture, Faisalabad 38040, Pakistan

³ School of Geography and the Environment, University of Oxford, Oxford, UK

⁴ School of Geography and Environmental Science, University of Southampton, Southampton SO17-1BJ, UK

Fig. 1 Map of the highlands of Yemen displaying the three catchments; a) Sana'a, b) Surdod, c) Siham, and names of local governorates situated within the region



Zone (RSCZ) and monsoonal Inter-Tropical Convergence Zone (ITCZ). The soil type can be described as sandy clay to clay loam with very low content of nutrients, while, shrubs and rangelands cover about 70% of the study area followed by built areas and agricultural fields. Rainfed agriculture is widely practiced and agriculture is critically dependent on irrigation from groundwater or from diverted streamflow and sheet flow (Alhakimi 2014). Sorghum and wheat are the periodic crops and Qat is the widely planted tree followed by grapes and coffee. Geologically,

the igneous and metamorphic basement rocks overlain by thick volcanic rocks and loess are the main features shaping the highlands of Yemen. The ancient terraces system, which were constructed at the beginning of the Bronze Age in the 3rd millennium BC is a unique feature of agriculture in Yemen. Across much of wadis, local people have constructed traditional earthen dams with small spillways to capture water from degraded mountain slopes, thereby creating terraces for cultivation. Over time, water-harvesting practices have gradually extended to the foothills of

the mountains, particularly in periods of increased aridity (Varisco 2019).

In the study area, agricultural terraces vary in scale and size. They can range from small, individual plots to large-scale terrace systems covering vast areas. The scale of terraces depends on the topography of the region and the specific needs of the farmers. Terraces are significantly present in the mountainous region where flat land is scarce (EPA 2013). Unfortunately, the terraces have faced significant degradation over time. Factors such as migration, urbanization, conflicts, and changing agricultural practices have contributed to the abandonment and deterioration of terraces (Weiss 2015). In parallel, the region is vulnerable to climate change and its impacts. Yemen is already facing significant water scarcity issues and real challenges in achieving food security under the limited freshwater resources and rapid population growth. Over three-quarters of the population resides in rural areas, engaging in farming and pastoralism as their primary occupations, while agricultural activities occupy over half of the available land (AL-Falahi et al. 2020). Climate change exacerbates these challenges by affecting agricultural productivity and increasing vulnerability of crops and livestock to severe weather incidents.

Further, the available projections of the climate change impacts across Yemen are coupled with a large uncertainty as most of conducted studies in Yemen relay on global climate models (GCMs) (Alderwish and Al-Eryani 1999; Al-Jibly 2008; Haidera et al. 2011; Haidera and Noaman 2010). Because of the coarse resolution of GCMs (> 100 km), the use of GCM output in hydrological models and for assessing climate change impacts at a local level (e.g., watershed) cannot be reliable (Saddique et al. 2019a, b; Gebrechorkos et al. 2019; Nasiri et al. 2020). In addition, there is a scarcity of historical climate data in Yemen, making it difficult to establish baseline climate conditions, identify long-term trends, and understand natural climate variability in the region (EPA 2013). Yemen's hydrological monitoring infrastructure is also insufficient, with a lack of well-maintained flow stations (van der Gun and Ahmed 1995).

The objective of the current study is to evaluate the performance of the Soil Water Assessment Tool and to assess the magnitude of water balance components under the potential impacts of climate change in the highland region of Yemen. The analysis employed flow monthly data from three catchments, namely *Sana'a* (flows to the east toward the desert zone); upland area of *Surdod* (excluding the coastal plain); and *Siham catchment* (both drain west into the Red Sea). The data were obtained from filed study documents of the national water resources authority (Nwra) for the period (1982–2000). The study utilizes data on daily rainfall, maximum and minimum temperature collected from 24 ground stations, supplemented by the most accurate satellite products specified on the region;

the Climate Hazards Group InfraRed Temperature with Station Data (CHIRTS); and Climate Hazards Group Infra-Red Precipitation with Station Data (CHIRPS). For assessing future climate changes, future scenarios produced by the Statistical Downscaling Model (SDSM), covering the period 2010–2100 under the Representative Concentrations Scenarios RCP2.6 and RCP8.5 were employed.

2 Material and methods

2.1 Description of the catchments

Sana'a catchment is located in the central part of the highland region (15.12°–16.0°N, 44.0°–44.50°E), flowing towards the east (Fig. 1). Its catchment area is 3,912 km², within an average elevation of 2,460 m. A substantial area of *Sana'a* catchment exhibits little or no vegetation cover. The estimated agricultural land is about 43,000 ha and much of it is rainfed (72%) and the rest depends on irrigation from groundwater. Based on the climate data used in this study (1981–2010), the long-term precipitation and temperature averages are 270 mm and 18 °C, respectively (Alwathaf and El Mansouri 2012).

Surdod catchment is the third-largest catchment situated within the region (15°–15.52°N, 43.4°–43.90°E). Running toward the Red Sea, *Surdod* contains several wadis and its catchment area is 2,400 km². The annual mean precipitation is 300 mm and the average temperature in the upper catchment is 18.2 °C. A considerable proportion of the cultivated land is predominantly confined to the valley floors, slopes, and irrigated terraces adjacent to stream channels. Much of the area along the *Surdod* catchment is under cultivation, while vegetation is lightly scattered across the upper reaches of *Surdod* catchment. The estimated arable land is 14,000 ha and most of it is rainfed agriculture (Alhakimi 2014).

Siham is one of the most fertile valleys of Yemen, as it irrigates many lands due to its convergence with the valleys of the northern country of Ans (Haidera et al. 2011; Alhakimi 2014). It is located (14.80°–15.24°N, 43.60°–44.32°E), nearly, in the southwest of the highland region occupying an area of 3,130 km². The mean annual rainfall is 280 mm and the average temperature is 18.3 °C. The mountains of *Siham* exhibit sparse and diffuse vegetation. The overall agricultural area is 92,843 ha, out of it 74,000 is rainfed and 20,000 is irrigated from runoff (Al Ward and Ismail 2019). Both *Surdod* and *Siham* are characterized by existence of terraces and rainwater harvesting structures (mainly in the upper land area) that collect the excessive rainwater in traditional storage for later use during drought (Haidera and Noaman 2010).

2.2 Soil and Water Assessment Tool (SWAT)

SWAT is a widely employed hydrological model used to evaluate water and land management practices and assess pollution discharges within complex watersheds (Al Khoury et al. 2023; Koltsida et al. 2023). It operates on a daily time step and considers climatic variables such as solar radiation, wind speed, temperature, precipitation, and relative humidity. Based on topographical features and flow networks, SWAT divides the catchment into subbasins, thus spatial heterogeneity in land use, soil and management practices is created (Zhang et al. 2019; Nasiri et al. 2020). Each subbasin contains Hydrologic Response Units (HRUs), which represent distinct zones with similar land cover and soil properties. The HRUs provide a more detailed representation of the watershed's heterogeneity (Mapes and Pricope 2020; Janjić and Tadić 2023).

SWAT computes reference evapotranspiration (ET_0) using several approaches such as Hargreaves, Priestley-Taylor, and Penman–Monteith. The method of choice is determined by the availability of pertinent meteorological data (Gebrechorkos et al. 2020). Computation of ET_0 was performed by Hargreaves method (Eq. 1) considering the limited data available from the study area (maximum and minimum daily temperature);

$$ET_0 = 0.0023 \cdot H_0 \cdot (T_{max} \sqrt{T_{min}})^{0.5} \cdot (T_{avg} + 17.8) \quad (1)$$

where:

ET_0 is the potential evapotranspiration in millimeters per day

H_0 is the extraterrestrial radiation in millimeters per day

T_{max} is the daily maximum air temperature in degrees Celsius

T_{min} is the daily minimum air temperature in degrees Celsius

T_{avg} is the average daily air temperature in degrees Celsius.

The surface runoff is calculated by examining contributory factors such as precipitation, land cover, soil properties, and topography (Nasiri et al. 2020). Different methods for estimating surface runoff are employed by SWAT, including the Green and Ampt and Soil Conservation Service (SCS) Curve Number (CN) method. The CN method is commonly used in SWAT for estimating surface runoff. This method assigns a curve number to different land cover types based

on their hydrological characteristics, such as infiltration capacity and runoff potential (Zhang et al. 2019).

To evaluate and quantify the other different aspects of the hydrological cycle, five hydrological components were selected. The Water Yield (WYLD); Evapotranspiration (ET); Surface Runoff (SURQ); Soil Water (SW); and the Groundwater Recharge (GW-RCH). The WYLD represents the total volume of water generated in the subbasin and HRUs that contributes to the mainstream channel (Kumar et al. 2017). The ET quantifies the amount of water lost from both the ground surface and through plants' transpiration. The SURQ refers to the portion of water that flows over the land surface. The SW accounts for the water stored within the spaces between soil particles. The GW_RCH reflects the amount of water infiltrating through the soil surface to replenish underground aquifers (Mapes and Pricope 2020).

We employed SWAT 2012, a hydrological simulation tool, to model the hydrological regime of the three catchments. The simulations were conducted using present-time data and climate future scenarios. For calibration purposes, we utilized SWAT-CUP, a specialized software package designed specifically for calibrating, conducting sensitivity analysis, and assessing uncertainties in the Soil and Water Assessment Tool (SWAT) model. Both SWAT 2012 and SWAT-CUP can be downloaded from <https://swat.tamu.edu/software>.

2.3 Datasets

2.3.1 Topography and watershed configuration

A 12.5-m spatial resolution Digital Elevation Model (DEM) is employed. The map, which is high-resolution and terrain-corrected, was acquired from the National Aeronautics and Space Administration (NASA) through their official website (<https://search.asf.alaska.edu>). SWAT utilizes the DEM for watershed boundary delineation and stream network generation. SWAT, further, uses the DEM to calculate the flow accumulation, which represents the accumulated flow from upslope areas to downstream locations (Saddique et al. 2019a, b).

2.3.2 Soil data

Soil classes in the three catchments were obtained from the World Soil Information (International Soil Reference and Information Centre (ISRIC)). ISRIC contains a wide range of soil-related data with different resolutions and depths from various sources around the world (<https://www.isric.org/>). Over the study area, four to five soil classifications with a 250 m spatial resolution are identified. Clay; clay loam; sandy loam; and sandy clay loam are the soil type dominating most the catchments area (Table 1). Loam and

Table 1 Proportional representation of soil characteristics across the three catchment (%)

Soil type	Sana'a catchment	Surdod catchment	Siham catchment
Clay loam	0.36	0.52	0.54
Sandy-clay loam	0.26	0.21	0.02
Loam	0.24	0.26	0.37
Sandy loam	0.14	0.005	0.001
Clay	—	0.004	0.06

Table 2 Distribution of land use and land cover in each catchment (%)

LULC	Sana'a catchment	Surdod catchment	Siham catchment
Water	0.07	0.02	0.01
Trees	0.02	0.001	0.03
Agricultural fields	0.24	0.15	0.21
Built area	0.16	0.05	0.1
Rangeland	0.47	0.74	0.62
Bare ground and grass	0.04	0.04	0.03

clay loam soil covers most of the high mountainous areas (63%), while sandy loam and sandy clay loam are the prevailing soil in the middle and low areas.

2.3.3 LULC data

Land use and land cover maps (LULC) generated from 30-m resolution Landsat 7 Enhance Thematic Mapper in 2000 is used during the calibration, and from the ESA Sentinel-2 imagery (Esri.Inc) at 10 m resolution produced by a deep learning model and published in January 2022 (<https://www.arcgis.com/home/item.html>), for the current and future time. The main land uses in the three watersheds are rangelands (> 60%), agricultural fields (20%), and built areas (10.4%). Compared to Siham and Surdod, a higher concentration of residential areas is found in Sana'a catchment due to location of the capital Sana'a and its suburbs within this watershed. Table 2 contains parentage of the land use and land cover area in the catchments;

Table 3 A list of hydrological stations used in this study and annual averages of precipitation and temperature across the catchments

Station	Area (km ²)	Location		Average annual rainfall (mm)	Average annual temperature (°C)
		Lat	Long		
Rahab (Sana'a)	3,912	15.98	44.43	270	18.0
Faj Al Hussen (Surdod)	2,400	15.18	43.41	320	18.2
Quatee (Siham)	3,130	14.85	43.72	290	18.3

2.3.4 Hydrometeorological information

Data on daily rainfall and temperature (1982–2000) from 24 stations; 9 in Sana'a; 8 in Surdod; and 7 in Siham catchment were employed for the hydrological modelling (Fig. 1). Due to some missing records in these stations, temperature and precipitation from CHIRTS and CHIRPS were utilized to complete and fill missing values. CHIRPS and CHIRTS datasets were identified as the superior performers when compared to ground station data (AL-Falahi et al. 2020). Other climate essential parameters such as wind speed, radiation, and relative humidity were adjusted using the weather generator component tool (CLIGEN) provided within SWAT. Monthly flow and runoff data from three stations (1982–2000) were provided by the National Water Resources Authority (NWRA), Ministry of Water and Environment and were used for SWAT calibration and validation (Table 3).

For future investigation of climate change impact on the hydrological regime, precipitation and temperature scenarios (2010–2100) generated by the Statistical-Downscaling Model (SDSM) under RCP2.6 and RCP8.5 are used. In the Sana'a catchment, 35 subbasins have been delineated whereas Surdod and Siham were, respectively, subdivided into 33 and 26 subbasins. The sub-basins were subsequently sub-divided into 252, 185, and 152 Hydrological Response Units (HRUs) for Sana'a; Surdod; and Siham catchment, utilizing slope, soil, and land use and land cover (LULC) incorporated maps in SWAT. Prior of generating the HRUs, the slope was defined into four classes (0–30%, 30–60%, 60–90%, and > 90%) and a 5% threshold value was applied in each sub-basin for each land use, soil type, and slope. By categorizing slopes into classes, SWAT can simulate the hydrological response for each class separately, allowing for a more accurate representation of watershed behavior.

2.3.5 Elevation bands and terraces integration

Great efforts were made to include these ancient water harvesting structures “**Terraces**” in the analysis. Prior to the inclusion of terraces in SWAT and for a more accurate representation of the topographical characteristics and their influence on hydrological processes, five elevation bands were defined at a subbasin level. Hence, variation in terrain

elevation is well-captured by SWAT. Subsequently, information about area size of terraces and location of terraces were collected from local reports and from a Yemeni agricultural map that shows agricultural area size at a local and district scale. The reports contained information about the percentage of terraces and flat fields as well as the pattern of irrigation. Using the LULC map (Sentinel 10 m resolution), overlapping LULC over the national map, and holding a direct overlook by using a satellite imagery from Google Earth and other maps as a visual reference to estimate the presence and distribution of terraces are the additionally applied methods. The work further included the use of measurement tools in Google Earth to estimate the dimensions of the identified terraces. Across the region, the terraces are present in the upper zone of Surdod and Siham watersheds, while Sana'a watershed does not have a considerable extent of terraces. Out of the total agricultural area, Surdod contained around 26% terraced fields in the catchment. Siham, on the other hand, has about 22.3% terraces area.

SWAT simulates terracing by adjusting slope length (HRU_SL), curve number value (CN), and erosion parameters (USLE_P). The slope length of a subbasin and HRUs should be set to a maximum distance between terraces (https://swat.tamu.edu/media/69398/ch33_input_ops.pdf). In sub-basins and HRUs where terraces are present, the slope length was set between 10–15 m and in some areas to 8 m length (very steep slope), depending on the slope degree and steepness of the terraced lands. To accommodate a modification in the curve number (CN), a zero of depth and mixing under the tillage operation was set to account for the ground cover developed by crops and rangelands. The CN and soil loss equations were modified according to the soil type and management practices. In the upper zones of Surdod and Siham watersheds, most of the soils are loam; clay loam; and sandy clay loam. SWAT use manual suggests values of P_factor, TERR_SL, and the curve number TERR_CN based on field slope, maximum slope length, and infiltration rate of the soil (S1, S2, and S3 table in the supplementary materials). Based on the defined four hydrologic soil groups (HSGs) along with management practices, a group B (moderate-low runoff potential and low infiltration), and C (moderate-high runoff potential and moderate infiltration), were selected to estimate changes in runoff resulting from terracing. Across much of subbasins and HRUs, the curve number (CN) was set at a range between 71–83.

The Universal Soil Loss Equation (USLE_P) is the parameter adjusted to estimate soil loss due to water erosion. Slope length, soil erodibility, rainfall erosivity, land management practices, and slope steepness (degree of slope) are the factors considered by the USLE (Duulatov et al. 2021). Terraces are effective in reducing soil erosion, so the P factor value for terraced areas should be lower compared to non-terraced areas (Deng 2021). This factor

was set between 0.16–0.23 considering the characteristics of terraces and the slope range of the area. In addition, SWAT's irrigation-from-reach feature was utilized to input data that controls the amount of water collected by different HRUs. Since the terraces may not be strategically positioned to capture all generated runoff within the sub-basin, the parameter flow fraction (FLOWFR) and maximum storage height (DIVMAX) were utilized to account for this side.

The proportion of runoff water that is captured by terraces and Hydrologic Response Units (HRUs) can be determined by the FLOWFR parameter. The maximum height of water storage on each terrace is regulated by the height of dikes and spillways, as well as the gentle slope of the land surface. This maximum storage height is denoted by the parameter DIVMAX (Ouessar et al. 2009). The FLOWFR for all terraces within a subbasin was kept constant based on the similar characteristics of the terraces throughout the subbasin. Given that not all runoff is captured by the terraces, the FLOWFR was set to 0.70 and to 0.85, while, the value of DIVMAX was set between 0.15 m to 0.30 m, based on our knowledge about average ponded water levels in terraces in Yemen.

2.4 Model performance metrics

During both the calibration and validation phases, graphical and statistical measurements were used to evaluate the hydrologic goodness-of-fit and overall performance of SWAT. The statistical criteria used were coefficient of determination (R^2), model efficiency or Nash–Sutcliffe coefficient (E), RMSE-observations standard deviation ratio (RSR), and percent bias (Pbias). The coefficient of determination (R^2) is a measure of the degree of linear correlation between the observed and simulated values. A value of R^2 close to 1, indicates a perfect match, and zero refers to a poor fit between the observed and simulated values. Nash–Sutcliffe illustrates how closely the observed vs. simulated data plot corresponds to the 1:1 line. The optimal value of Nash–Sutcliffe is 1 (Gebrechorkos et al. 2020). RSR values ranging from 0.0 to 0.5 indicate excellent performance. The lower the RSR number, the lower RMSE normalized by the standard deviation of observations. Systematic deviation of the simulated values to consistently overestimate or underestimate the observed values is assessed by the Pbias. Pbias near or close to 0.0 indicates an accurate model simulation. Overestimation is indicated by a positive Pbias, whereas underestimating is shown by a negative Pbias (S. H. Gebrechorkos 2019; Nasiri et al. 2020). These statistics are the most often used measures in hydrological models' calibration and validation.

$$R^2 = \frac{(\sum_{i=1}^n (O_i) - (O_{avg}))^2}{\sum_{i=1}^n (O_i - O_{avg})^2 \sum_{i=1}^n (S_i - S_{avg})^2} \quad (2)$$

$$NSE = 1 - \frac{\sum_{i=1}^n (O_i - S_i)^2}{\sum_{i=1}^n (O_i - O_{avg})^2} \quad (3)$$

$$RSR = \frac{RMSE}{SD_{obs}} = \frac{\sqrt{\sum_{i=1}^n (O_i - S_i)^2}}{\sqrt{\sum_{i=1}^n (O_i - O_{avg})^2}} \quad (4)$$

$$PBIAS = \frac{\sum_{i=1}^n (S_i - O_i)}{\sum_{i=1}^n O_i} \times 100 \quad (5)$$

where S_i represents the simulated discharge, O_i denotes the observed discharge, O_{avg} , and S_{avg} represent the mean of observed and the simulated discharge, respectively, and n is the number of data records.

3 Results

3.1 Sensitivity analysis

Prior to model calibration, parameters sensitivity analysis was carried out using SWAT-CUP. The sensitivity analysis assesses the model's response to changes in input parameter values. The evaluation assesses the impact of variations in the baseline model parameter values on the water balance components. Therefore, it identifies the parameters that exert the most significant influence on the outflow of the three watersheds (Kumar et al. 2017; Khelifa et al. 2017). The parameters used for sensitivity analysis in this study were selected according to the model description and previous applications of SWAT found in published literature (Achamyeleh 2019; Nasiri et al. 2020), while the global sensitivity analysis (GA) was utilized on the grounds of its competence to propagate all uncertainties and identify the key parameters that affect model performance. During the calibration, SWAT was run 9000 times and 4 iterations were carried out in each catchment. For the three catchments, 19 parameters were chosen to simulate historical discharges. The most sensitive parameters, based on the p-value (smaller value) and t-statistic (larger value), are: SCS runoff curve number (CN2); Manning's value for the main channel (CH_N2); base flow alpha factor (ALPHA_BF); effective hydraulic conductivity in main channel alluvium (CH_K2); plant uptake compensation factor (EPCO); soil evaporation compensation factor (ESCO); depth of water in shallow aquifer to return flow from groundwater (GWQMN); universal soil

loss equation (USLE); slope subbasin (SLUBBASN); Flow fraction (FLOW_FR); and height of the terrace (DIVMAX). The four later parameters were employed in the upstream zone of Surdod and Siham catchment where terraces exist. In each model run, the model parameters ranges were manually adjusted through a trial-and-error process. The adjustment was performed using the statistical indicators within the model to achieve a closer match between the simulated discharge and the observed discharge (Ouassar et al. 2009). Table 4 contained the list of the most sensitive selected parameters;

3.2 Result of calibration and validation

The SUFI-2 algorithm was employed within the SWAT-CUP framework for SWAT model calibration and validation. Monthly flow data recorded on 1985 to 1995 were utilized for calibration, while the validation utilized data for the period between 1996 and 2000. A warm-up period of three years (1982–1984) was implemented before running the model. Prior to calibration, meticulous updates were made to all pertinent parameters and input data, including soil properties, land use/land cover (LULC) information, slope characteristics, hydro climate data, and the inclusion of terraces. These updates were critical to ensuring the modeling consistency and dependability. For validation, the calibrated parameters (Table 4) were employed with the independent datasets (1996–2000) that were not used in the calibration process to evaluate the capability of SWAT in generating an accurate discharge beyond the calibration period. Overall, SWAT demonstrated high performance in capturing the relationship between rainfall and local discharges in the three catchments. In Sana'a catchment, during the calibration, the R^2 , NSE, RSR, and Pbias values were 0.82, 0.74, 0.51, and -8.7, respectively. For validation, these values slightly decreased to 0.76, 0.66, 0.58, and -13.4 for R^2 , NSE, RSR, and Pbias, respectively. The P-factor and R-factor, which indicate model accuracy (% of observed data enclosed by the modeling output) and model uncertainty (95PPU), were determined as 0.76 and 0.21, respectively. During the dry period (winter months), the Pbias value between observed and simulated was -5.3 compared to -19.2 in the wet period. A similar outcome was nearly observed within the Surdod catchment area. The R^2 , NSE, RSR, and Pbias values were respectively 0.89, 0.83, 0.50, and -9.7 in the dry period. During the rainy months, the R^2 , NSE, RSR, and Pbias showed values of 0.87, 0.79, 0.54, and -12.7, respectively. For the Siham watershed, the assessment results during the dry time were R^2 : 0.81, NSE: 0.78, RSR: 0.45, and Pbias: -9.6. During the rainy seasons, the corresponding values were 0.80, 0.81, 0.49, and -13.8 for R^2 , NSE, RSR, and Pbias, respectively. The P-factor and R-factor were determined as 0.83 and 0.17 for Surdod, and 0.87 and 0.11

Table 4 List of parameters and their ranges used for SWAT calibration

No	Parameter	Initial range	Sana'a catchment	Surdod catchment	Siham catchment
1	r_CN2.mgt	±0.25	0.12	0.10	0.11
2	v_GW_DELAY.gw	0–500	95.7	97.5	136.2
3	v_GW_REVAP.gw	0.02–0.2	0.12	0.09	0.15
4	v_REVAPMN.gw	0–500	315.7	322.5	285.59
5	v_RCHRG_DP.gw	0–1	0.42	0.59	0.60
6	v_ALPHA_BF.gw	0–1	0.61	0.90	0.17
7	v_CH_K2.rte	0.001–200	73.8	83.2	78.53
8	v_CH_N2.rte	-0.01–0.3	-0.1	0.13	0.21
9	v_EPCO.hru	0–1	0.05	0.19	0.21
10	v_ESCO.hru	0–1	0.10	0.29	0.37
11	r_SOL_AWC.sol	±0.20	0.040	0.10	0.10
12	r_SOL_K.sol	±0.20	-0.83	0.09	0.08
13	v_GWQMN.gw	0–5000	4500	4200	4000
14	v_ALPHA_BNK.rte	0–1	0.43	0.81	0.35
15	r_SOL_BD.sol	0.9–2.5	0.3	1.51	1.37
16	v_USLE_P	0–1	-	0.23	0.16
17	v_SLUBBSN	5–150	-	5–10	5–15
18	v_FLOW_FR	0–1	-	0.70–0.85	0.70–0.85
19	v_DIV_MAX	0–150	-	0.15–0.30	0.15–0.30

r_ signifies that the existing parameter value is multiplied by a specific factor, typically (1 + a given value); v_ indicates that the default parameter is replaced entirely with a predetermined value

for Siham, respectively. Calibration and validation result of SWAT are shown in Fig. 2 below.

To assess the model's accuracy and determine if terraces have a major influence on the flow regime, calibration of SWAT was additionally conducted in Surdod and Siham watershed, excluding terraces. The statistical indicators used for the evaluation, namely R^2 , NSE, RSR, and Pbias, yielded average values of 0.74, 0.63, 0.61, and -20.3, respectively. The computed average P-factor and R-factor values for both catchments were 0.64 and 0.29, respectively. These results indicate a relatively lower performance of SWAT model when compared to the previously discussed outcomes that incorporated terraces. During the test period (1985–2000), the discharge in Surdod reduced from 94 m³/s to 78.2 m³/s after terraces were introduced to SWAT. Siham, on the other hand, showed a decrease in the flow out (discharge) to 69.4 m³/s compared to 82.7 m³/s when terraces were not included.

3.3 Climate change potential impact on the region

The performance of SDSM in generating estimates compared to observed data was evaluated using the metrics discussed in Section 2.4. The SDSM model showed a higher accuracy in synthesizing T-max, T-min, and precipitation estimates. In the three catchments, SDSM showed an averaged R^2 of 0.82 for precipitation, 0.88 for maximum temperature, and 0.87 for minimum temperature (Fig. 3). The averaged RMSE was 1.6 for precipitation, 0.2 for maximum

temperature, and 0.15 for minimum temperature. SDSM showed an averaged Pbias of 5.4 for maximum temperature, 3.5 for minimum temperature, and 5.7 for precipitation. The highest R^2 value for precipitation was found in Al Hayfah station in Sana'a catchment ($R^2 = 0.92$), Assalf station in Surdod ($R^2 = 0.96$), and Haraz station in Siham ($R^2 = 0.93$). The RMSE and Pbias showed lower values in Al Hayfah and Hinadi, Haraz, and Assalf stations in Sana'a, Siham, and Surdod catchment, respectively. Overall, the performance of SDSM demonstrated a predictive skill in reproducing historical observations and it is applied to develop future climate scenarios from GCMs in the study area.

Based on SDSM, the region is projected to experience higher precipitation more than 340 mm of annual averages the amount observed in the baseline period (1981–2010). The projected increase of the precipitation is 20% in 2011–2040 (2020s), 28.2% during 2041–2070 (2050s), and up to 40.81% in 2071–2100 (2080s), respectively. The most significant increase in seasonal precipitation is projected under RCP8.5 in the 2080s, particularly in the western zones of the region during March to May (MAM), June through August (JJA), and in autumn from September through November (SON) across the eastern districts. Under the RCP8.5 scenario, it is projected that certain areas within the western districts, mainly Al Rojoun, Al Mahwit city, and Al Khabt in Al Mahwit governorate; Haraz, Al Haymah, and Bani Mattar in Sana'a governorate; and Algabin in Raymah governorate will experience an approximate 18%

Fig. 2 Result of calibration and validation of SWAT relative to monthly observed discharge (cms) in the three catchments

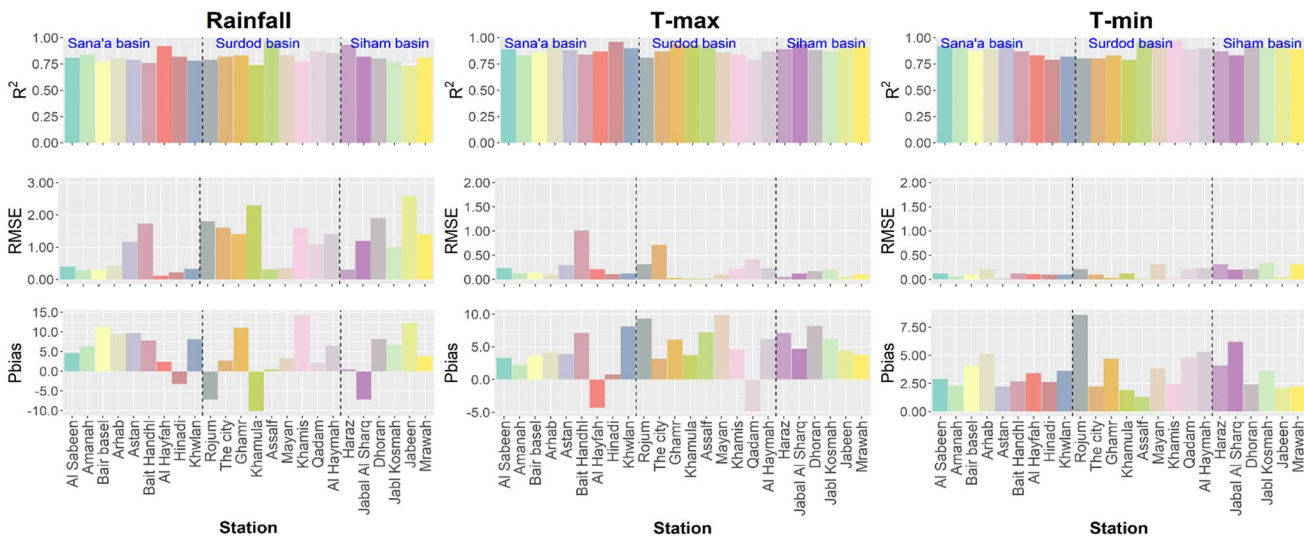
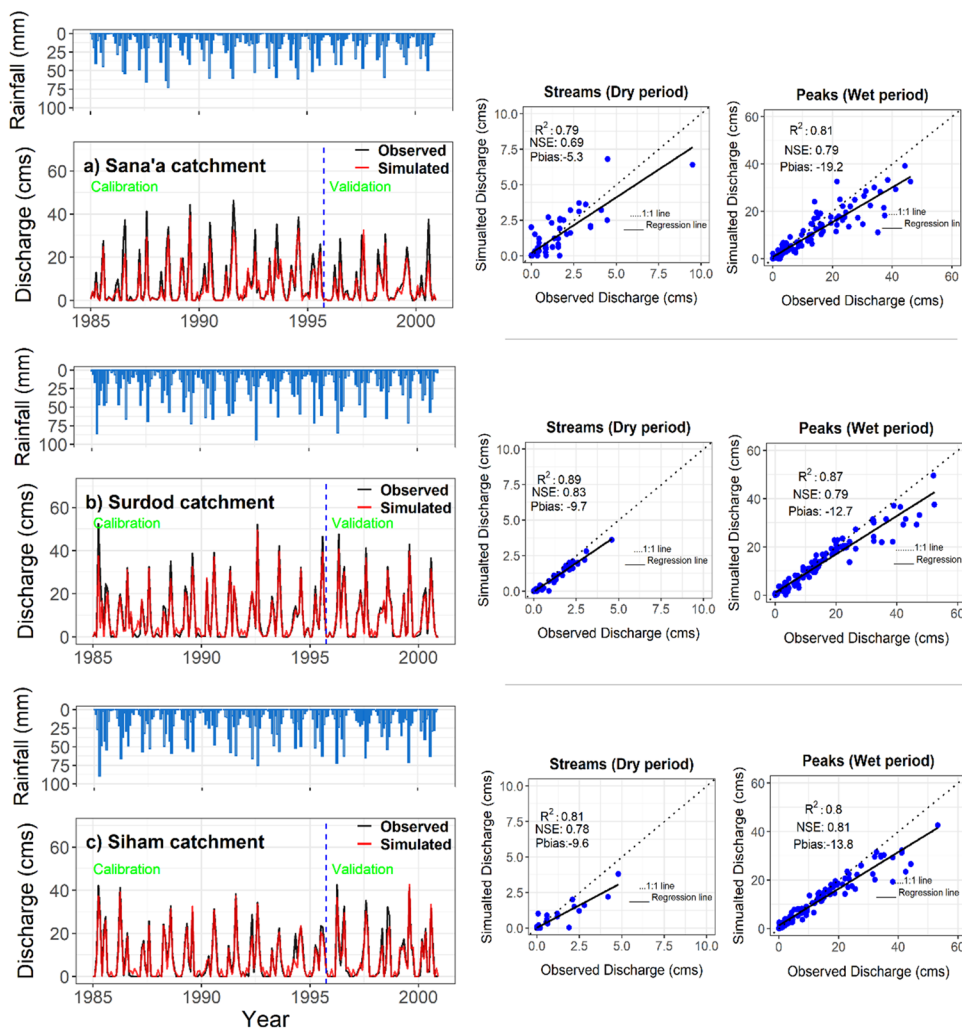


Fig. 3 Result of the statistical evaluation of SDSM output against monthly observations (1981–2010) in the three basins. Left column displayed the result of precipitation, maximum temperature (middle

column) and the minimum temperature's statistical results are shown in the right column

increase in precipitation rates during the dry period (DJF) in the 2020s and 2080s. Furthermore, T-max (T-min) temperatures are projected to rise by up to 0.4 °C (0.5 °C), 0.7 °C (0.6 °C), and 1.1 °C (0.9 °C) in the 2020s, 2050s, and 2080s, compared to the current time annual averages of 23.2 °C for T-max and 10.9 °C for the T-min (Fig. 4).

In Sana'a watershed, the percentage of precipitation change showed an increase in annual average of > 14.45% and 24.6% under RCP2.6 and RCP8.5, respectively. T-max (T-min) will be warmer than the reference period by more than 0.41 °C (0.36 °C), 0.52 °C (0.44 °C), 0.71 °C (0.50 °C), 0.92 °C (0.71 °C) in the 2020s and the 2080s under RCP2.6 and RCP8.5, respectively. The annual average projected precipitation showed an increase in Surdod and Siham up to 18.2% and 36.2% under RCP2.6 and RCP8.5, respectively. The T-max (T-min) will rise in Surdod up to 0.70 °C (0.57 °C) in the 2020s and up to 0.84 °C (0.76 °C) in the 2080s. In Siham catchment the projected increase of T-max and (T-min) is 0.87 °C (0.89 °C) and 1.3 °C (0.98 °C) in the 2020s and the 2080s, respectively.

3.4 Impact assessment of hydrological regime of the region

3.4.1 Sana'a catchment

The average seasonal flow throughout the Sana'a basin is expected to increase during the long rainy season (JAS) with highest increase occurring in September. The most pronounced increase is found under RCP8.5 in the 2080s up to 19.6%. Under RCP2.6, an increase in the flow of up to 10% and 14% is projected during the 2020s and 2080s, respectively. The increase is considered negligible during the short rainy season (MAM), most likely due to reduced predicted precipitation. The projected increases in precipitation will result in high annual increases of the hydrological components across Sana'a catchment. Compared to an average of 2.6 mm in the baseline period, the WYLD will increase under RCP2.6 by up to 5.6% and 7.8% in the 2020s and 2080s, respectively.

The RCP8.5 demonstrates a higher increase in WYLD up to 8.3% and up to 9.7% in the 2020s and 2080s. The upper high-elevation zones show the most significant increase in WYLD, primarily due to the higher projected precipitation and the steep terrain in this part of the catchment. The SURQ will increase up to 4.3% and 4.6% under RCP2.6, up to 5.7% and > 7% under RCP8.5 for the 2020s and the 2080s, respectively. The projected increase in ET is the greatest among the other examined variables, which show an increase up to 14.3% and 17.6% under RCP2.6, and up to 12.7% and 28.9% under RCP8.5 in the 2020s and 2080s, respectively (Fig. 5).

Further, the SW and GW_RCH exhibit varying rates of increase in the future, with the highest rates in the 2080s under both RCPs. The SW is expected to increase by up to 3.4% and 3.6% under RCP2.6 in the 2020s and 2080s, respectively. Under RCP8.5, the projected increase in SW is estimated to be 3.9% and 4.9% in the 2020s and 2080s. GW_RCH is projected to increase by up to 3.2% and 4.6% under RCP2.6, and up to 4.8% and 10.8% under RCP8.5 in the 2020s and 2080s, respectively. The increased precipitation has an impact on SW and GW_RCH with greater rates predicted in sub-basins and hydrologic response units (HRUs) with clay and clay loam soils.

In contrast, sub-basins consisting of sandy clay soils exhibit relatively higher rates of GW_RCH. Gently sloping terrains, especially in basins situated at the foothills of nearby mountains, exhibited higher levels of GW_RCH, which could be attributed to the increased runoff originating from the mountainous areas in the upper subbasins. Further, sub-basins in urban and built-up regions such as Sana'a have the lowest levels of both SW and GW_RCH (Table 5).

3.4.2 Surdod catchment

Under both RCPs, the average seasonal flow in Surdod is expected to increase in the 2020s, 2050s, and 2080s. Based on the GWQ analysis, an increase in seasonal flow is projected up to 6.6% and 11% under RCP2.6, and up to 9% and 17% under RCP8.5 for the 2020s and 2080s, respectively. The increase in wadi flow is more pronounced in MAM and

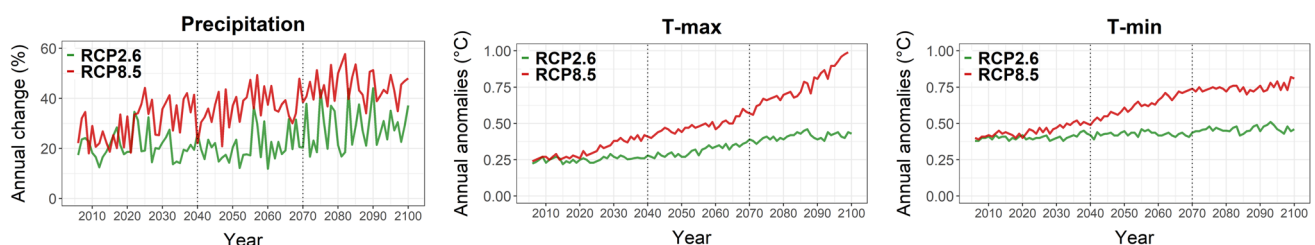


Fig. 4 Annual anomalies of T-min (°C), T-max (°C), and change of precipitation (%) in the study area. Prior to using the climate future projections in simulating future change in discharge, the output of

SDSM under RCP2.6 and RCP8.5 were bias-corrected applying Quantile Mapping method (QM)

Fig. 5 Spatial distribution of relative change rate (%) of water components under RCP2.6 and RCP8.5 across Sana'a catchment

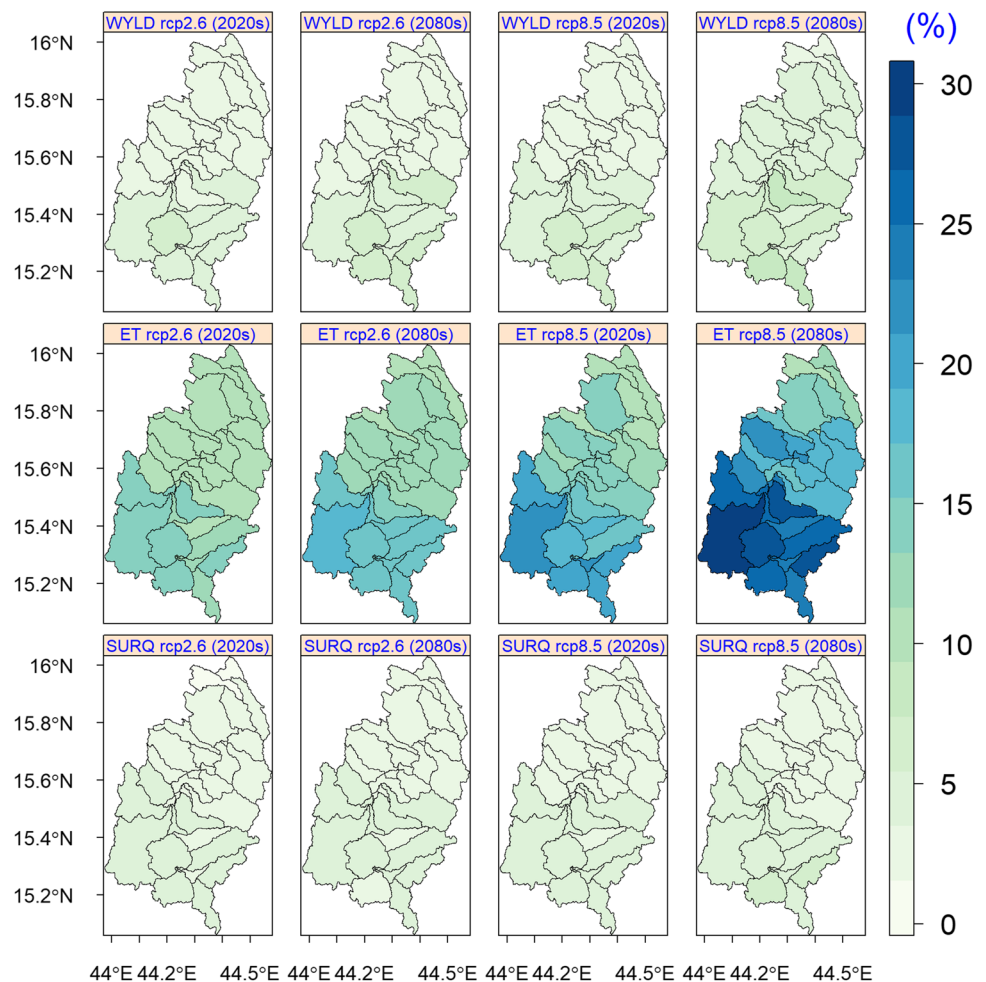


Table 5 Comparative analysis of long-term changes in average annual precipitation (%), minimum temperature ($^{\circ}\text{C}$), maximum temperature ($^{\circ}\text{C}$), flow (%), total soil–water (%), and evapotranspiration (%) in the 2020s and 2080s under the RCP2.6 and RCP8.5 in Sana'a catchment compared to the baseline period

Catchment	Variable	RCP2.6		RCP8.5	
		2020s	2080s	2020s	2080s
Sana'a	Precipitation	11.7	16.2	13.3	29.9
	Maximum temperature	0.41	0.52	0.71	0.92
	Minimum temperature	0.36	0.44	0.56	0.71
	Flow	8.2	11.1	12.9	18.2
	WYLD	5.6	7.8	8.3	9.7
	ET	14.3	17.6	12.7	28.9
	SURQ	4.3	4.6	5.7	7.3
	SW	3.43	3.6	3.9	4.9
	GW_RCH	3.2	4.6	4.83	10.8

JAS. During DJF, a relative rise in the base flow is also projected as a result of the increased precipitation during the dry season, particularly in the 2080s under RCP8.5.

Compared to the historical period, the annual average of WYLD is projected to increase up to 7.2% and 9.3% under RCP2.6 in the 2020s and 2080s, respectively. Under RCP8.5, the projected increase is about 9.9% and 12.1% during the 2020s and 2080s. In the upper zone area of Surdod, the WYLD is lower compared to the projected estimates in the subbasins where no terraces are present, despite receiving nearly identical amounts of precipitation. This lower quantity of the projected WYLD in the upper zones of Surdod could be affected by terraces that retain a large portion of the flow from reaching the stream main channel. Further, the lower projected estimates of precipitation in some downstream subbasins affect the levels of WYLD in comparison with the upstream zones.

The SURQ shows an increase up to 4.9% and 10.3% under RCP2.6, and 11.2% and 14.6% under RCP8.5 for the 2020s and 2080s, respectively. Similar to the WYLD results, subbasins and terraced HRUs in the upper lands of Surdod showed lower levels of SURQ under both RCPs in the 2020s and 2080s. This could conclude that the WYLD and SURQ are both affected by presence of terraces. In general, the most substantial increase across Surdod watershed is observed in

the evapotranspiration (ET) component, especially in the terraced lands. Under RCP2.6, the ET is expected to increase by more than 17% in the 2020s and by 20% in the 2080s. For RCP8.5, the projected increase in ET is up to 20.4% in the 2020s and 29.1% in the 2080s. Moreover, several sub-basins and HRUs, mainly those located in the middle zone of Surdod, showed high rate of ET as well, which can be influenced by the increased precipitation levels on this zone and presence of vegetation cover (Fig. 6).

Further, the projected increase of GW_RCH is 5.3% and 6.4% under RCP2.6, and up to 7.41% and 9.4% by RCP8.5 in the 2020s and the 2080s, respectively. The SW projected increase is about 3.9%, and 4.7% as observed under RCP2.6, and up to 4.52% and 5.9% by RCP8.5. Table 6 illustrates the projected changes in the averages of the examined water balance components and climate variables;

3.4.3 Siham catchment

Seasonal flow in Siham is projected to increase in the future. In MAM an increase is projected up to 6.3% and 9.2% under RCP2.6 and up to 12.1% and 15.3% by RCP8.5 in the 2020s and 2080s, respectively. During JAS about 13.4% and 15% is the projected increase by RCP2.6. Under

Table 6 Comparative analysis of long-term changes in average annual precipitation (%), minimum temperature ($^{\circ}$ C), maximum temperature ($^{\circ}$ C), flow (%), total soil-water (%), and evapotranspiration (%) in the 2020s and 2080s under the RCP2.6 and RCP8.5 in Surdod catchment compared to the baseline period

Catchment	Variable	RCP2.6		RCP8.5	
		2020s	2080s	2020s	2080s
Surdod	Precipitation	12.7	18.7	26.2	36.6
	Maximum temperature	0.67	0.78	0.80	1.2
	Minimum temperature	0.52	0.69	0.92	0.96
	Flow	11.3	15.1	14.6	22.3
	WYLD	7.2	9.3	9.9	12.1
	ET	17.2	19.9	20.4	29.1
	SURQ	4.9	10.3	11.2	14.6
	SW	3.9	4.7	4.52	5.9
	GW_RCH	5.3	6.4	7.41	9.4

RCP8.5 the projected increase is 14.6% and 18% in the 2020s and 2080s, respectively. The annual averages of the WYLD will increase in the 2020s and the 2080s up to 7.3% and > 10% under RCP2.6, and to about 9.7% and 11.4% under RCP8.5.

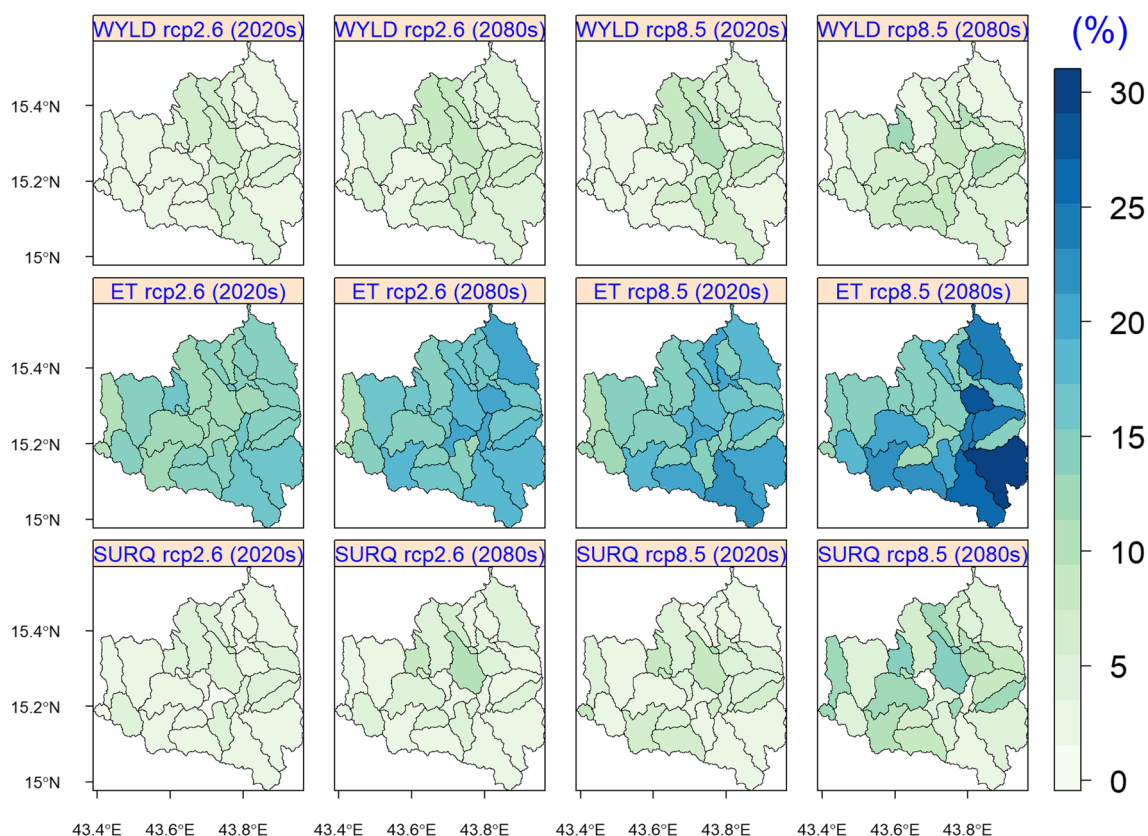


Fig. 6 Spatial variation of relative change rate (%) in the WYLD, ET and the SURQ in Surdod catchment area under RCP2.6 and RCP8.5

An increase of 4.3% and 8.6% is projected in the SURQ under RCP2.6 and up to 10.2% and 13.7% by RCP8.5, respectively. Similar to Surdod, WYLD and SURQ levels are affected by presence of terraces. Further, the ET is anticipated to be higher in the future up to 15.2% and more than 17% under RCP2.6 and up to 19.4% and 27.8% by RCP8.5 in the 2020s and 2080s, respectively (Fig. 7).

Levels of SW will increase up to 2.1% and 2.9% under RCP2.6, and up to 5.1% and 7.02% by RCP8.5 in the 2020s and the 2080s, respectively. The expected increase in GW_RCH is 3.2% and 4.1% under RCP2.6, and up to 5.9% and 10.13% by RCP8.5 in the 2020s and the 2080s. In general, the terraced lands exhibit relative higher SW compared to the flat areas, whereas the GW_RCH rates are greater in the adjacent subbasins that are located in the gentle slope directly downstream of the upper land basins. Change in the averages of the water balance investigated components in Siham catchment are shown in Table 7.

4 Discussion

High-resolution data are essentially required to assess the potential impacts of climate change on water balance components. Global Climate Models (GCMs) face biases, encounter significant uncertainties, and require extensive computational methods and resources to project future climate conditions (Homsí et al. 2020). In contrast, techniques

Table 7 Comparative analysis of long-term changes in average annual precipitation (%), minimum temperature (°C), maximum temperature (°C), flow (%), total soil–water (%), and evapotranspiration (%) in the 2020s and 2080s under the RCP2.6 and RCP8.5 in Siham catchment compared to the baseline period

Catchment	Variable	RCP2.6		RCP8.5	
		2020s	2080s	2020s	2080s
Siham	Precipitation	12.3	17.3	23.4	29.2
	Maximum temperature	0.72	0.89	0.94	1.4
	Minimum temperature	0.61	0.83	0.86	1.0
	Flow	8.9	11.2	13.3	20.7
	WYLD	7.3	10.2	9.7	11.4
	ET	15.2	17.5	19.4	27.8
	SURQ	4.3	8.6	10.2	13.7
	SW	2.1	2.9	5.1	7.02
	GW_RCH	3.2	4.1	5.9	10.13

such as statistical downscaling offer enhanced spatial and finer temporal resolution data, making them more reliable for local scale applications compared to the information supplied by Global Climate Models (GCMs) (Gebrechorkos et al. 2019). The Statistical Downscaling Model (SDSM) is commonly used to mitigate uncertainties facing GCMs (Hashmi et al. 2011; Hassan et al. 2014; Tahir et al. 2018; Al-Mukhtar and Qasim 2019; Gebrechorkos et al. 2019; Dehghan et al. 2020; Lotfi et al. 2022). This

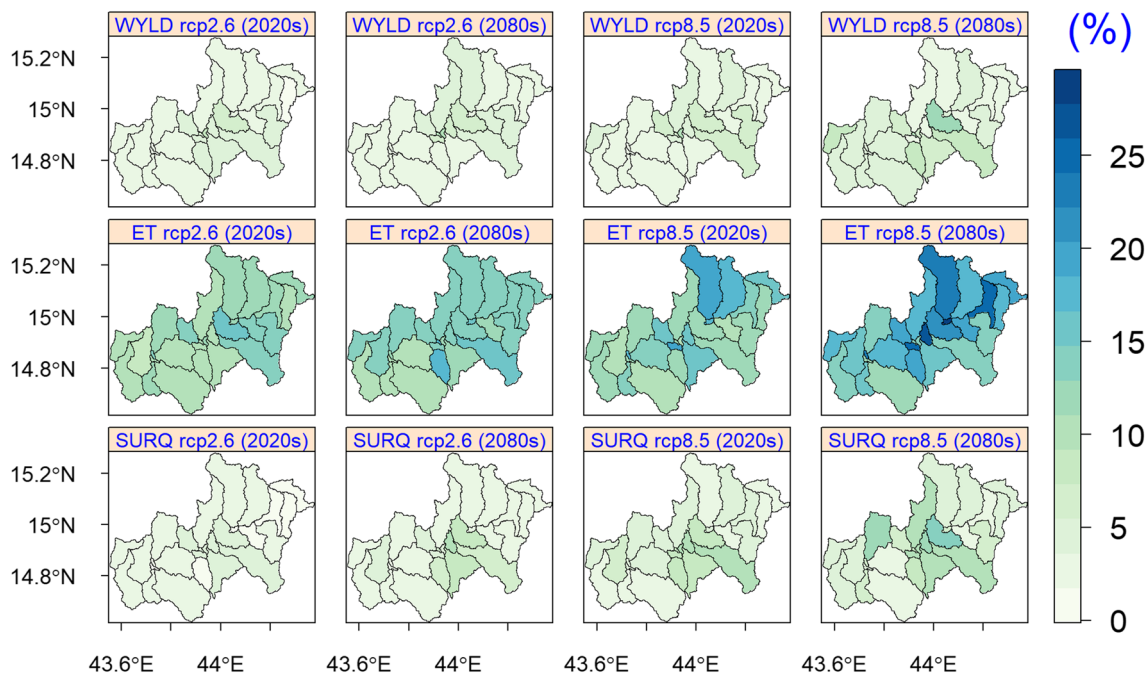


Fig. 7 Spatial distribution of the percentage change rate of the water components under the RCP2.6 and RCP8.5 scenarios throughout the Siham catchment

approach combines GCMs predictors with observational data (predictands) and offers a simple but yet practical means of downscaling to finer resolutions, thereby minimizing uncertainties encountered by the GCMs. The application of the SDSM is widespread in downscaling climate variables such as precipitation, maximum temperature, and minimum temperature for impact assessment studies at local and regional scales (Al-Mukhtar and Qasim 2019; Abdulla 2020; Dehghan et al. 2020; Lotfi et al. 2022).

Across the study area, the SDSM was employed to down-scale climate data for the present (1981–2010) and future (2011–2100) climatic periods. The SDSM demonstrated an outstanding representation of the observed historical data during the calibration and validation, confirming consistency with other studies (Tahir et al. 2018; Gebrechorkos et al. 2019; Saddique et al. 2019a, b). In the meantime, the Soil and Water Assessment Tool (SWAT) was employed to study the impact of climate future changes on the hydrological regime of the highland region of Yemen utilizing the outcome of SDSM. SWAT has been used in humid, arid, and semi-arid climates (Abbasnia and Toros 2016; Klaas et al. 2018; González-Rojí et al. 2019; Tukimat et al. 2019) and showed high performance in assessment studies conducted at a watershed scale.

In this study and in order to assess the effects of terraces on the calibration results and hydrological response, mainly in Surdod and Siham catchments where terraces exist, SWAT was examined with and without the integration of terraces. The modelled discharge using SWAT showed high agreement with the observed discharge during the calibration (1982–1995) and the validation (1996–2000) periods in Sana'a catchment. Further, SWAT demonstrated a very good performance in Surdod and Siham watersheds. After incorporating terraces into the model and making the necessary parameter adjustments, SWAT exhibited enhanced performance compared to the situation before inclusion of terraces. According to Moriasi (2015), the result of calibration results before and after the introduction of terraces were very good and satisfactory (S4, supplementary materials), respectively.

The increased temperature and precipitation are associated with an increase in various hydrological variables such as discharge, WYLD, ET, SURQ, SW, and GW_RCH. Majority of the increase is projected under RCP8.5 during the 2080s. Further, the projected rise in temperature is likely to result in a substantial contribution from the ET component to the overall projected precipitation in the three catchments.

In Sana'a catchment, the upstream subbasins are projected to experience higher rates of WYLD as a result of the projected increase in precipitation in this zone compared to the downstream sub-basins under both RCPs. Further, SURQ is projected to increase in the three catchments. Compared to

Sana'a catchment, Surdod and Siham are projected to experience higher precipitation and subsequently will produce greater runoff. Because of the steep slopes in the mountainous areas of Siham and Surdod catchments accompanied by limited water infiltration capacity of the rocky and the shallow soils, a great amount of rainfall becomes runoff rapidly (Alhakimi 2014).

The topographical characteristics (sloping area) of Surdod and Siham catchments, soil type, land use, and management practices all contribute to generation of more surface runoff as a response to the increased precipitation. This outcome is consistent with earlier studies conducted in Yemen (Haidera et al. 2011; Alhakimi 2014). We have also observed that certain factors that fall beyond the scope of this study such as the increase in vegetation cover during the rainy season as well as variation of the vegetation cover in the wet and dry years are also expected to exert an influence on the runoff dynamics. Moreover, the presence of water harvesting structures (**terraces**) in the Surdod and Siham watersheds appears to have a substantial impact on the levels of ET, WYLD, and SURQ.

The terraced subbasins exhibit high rates of ET and relatively lower levels of WYLD and SURQ. The high level of the projected ET in the terraced subbasins can be attributed to the presence of multiple terraces or steps that create a larger surface area compared to flat fields. The increased surface area exposes more soil to sunlight and airflow, leading to enhanced evaporation and transpiration processes (Wang 2021). Furthermore, terraced fields often have better water retention capabilities compared to flat fields, allowing for better water infiltration and reduced runoff. Thus, crops and plants in terraced fields have more access to soil moisture, which promotes higher evapotranspiration rates. Studies conducted in Tunisia (Khelifa et al. 2017) and Ethiopia (Worku et al. 2020) suggest a reduction in surface runoff because of terraces by approximately 19% and 25%, respectively.

The GW_RCH and SW are projected to experience a comparatively smaller increase. Compared to Surdod and Siham, Sana'a catchment exhibited higher levels of GW_RCH. This could be related to various factors including the presence of permeable soil and alluvium deposits, shallow nature of the soil, and due to the large area of Sana'a catchment. According to Masoud et al. (2018) the average annual groundwater recharge in Wadi Baysh (Saudi Arabia) is 72 mm, based on infiltration and intensive field pumping tests. This result agrees with the conclusion obtained from SWAT, which indicates around 17% of the total precipitation falling on Sana'a catchment contributes to groundwater recharge.

Within Surdod and Siham watersheds, the subbasins that are characterized by high-infiltration soil, such as sandy loam and sandy clay loam, as well as subbasins located at the base

of mountainous terrain including alluvial beds, have exhibited higher rates of GW_RCH. In the terraced fields as well as the subbasins that are dominated by clay loam and loam soil, levels of SW were comparatively higher. However, certain subbasins within the clay and loam soil displayed relatively lower levels of SW, possibly due to the lower estimates of the projected precipitation on these subbasins. Generally, the percentage of simulated GW_RCH by SWAT (17%) agrees with the conclusion of several studies conducted in the semi-arid environments, which reported annual recharge rates ranging from 4.8% to 15% (Jafari 2019) and up to 32% (Melki 2017) of the total precipitation. Also, the considerable changes in most of the hydrological variables in the three catchments, particularly in the 2080s are aligned with the expected change in greenhouse gas emission (IPCC 2022).

In the study area, the projected increase in Wadi flows and total soil water in the three catchments will provide substantial support to essential sectors such as agriculture and water resources. Given that the greatest magnitudes of the Wadi flow-projected increase will occur in the 2080s under RCP8.5, the Yemeni government needs to consider implementation of flood protection measures in multiple subbasins. With the increasing impact of flood hazards, many studies emphasize the significance of adopting integrated flood management practices in the future. Enhancing effective collaboration between the community and stakeholders and developing a diverse set of flood management frameworks are of primary importance for better flood risk management. Other research suggests both extending the retention system and distributed storage as an effective measure to mitigate the impact of floods. Enhancing preparedness, constructing new dams, implementing rainwater harvesting initiatives in rural and urban areas, and modernizing pertinent organizations and institutions are primary strategies to mitigate the effects of flood in a semi-arid region.

On the other hand, groundwater levels in Siham are relatively shallow compared to Surdod and Sana'a. Increased precipitation may enhance the recharge rates and replenish the shallow groundwater reservoirs. The variation in SW levels across the subbasins is generally not significant, likely due to the predominant soil type (clay loam to loam) throughout Siham catchment. Therefore, it can be concluded that levels of SW are exclusively influenced by the projected precipitation estimates between the upstream and downstream areas as well as by the existence of water harvesting structures in the upper land areas.

5 Conclusion

A combination of hydrological and climatic modeling is used to assess the influence of future climate on water balance components in Yemen's highlands. The research

focused on two terraced watersheds (Surdod and Siham) and a flat to semi-flat watershed (Sana'a). Selection of the catchments was driven by their significant socioeconomic and ecological importance, as well as the availability of historical hydrological data. SDSM results suggest an increase (> 28%) in precipitation in Sana'a, (> 36%) in Surdod, and (29.2%) in Siham catchment throughout the twenty-first century. Moreover, T-min and T-max will be higher than the baseline period (1981–2010). As a consequence, streamflow, total soil–water, and evaporation exhibit a visible increase during the 2020s, 2050s, with a greater increase in the 2080s under RCP8.5.

SWAT results reveal an increase in seasonal flow in Sana'a up to 10% during JAS in the 2020s under RCP2.6 and up to 14% in the 2080s. This can be a temporary streamflow during the JAS, which may extend to the following months after significant rainfall events. Under the RCP8.5, the seasonal flow is projected to increase up to 19% and up to 22% in the 2020s and 2080s, respectively. Streamflow in Siham will increase during MAM as well as in the JAS up to 9.9% and to 12.1% under RCP2.6 in the 2020s and by up to 13.4% and up to 16.7% under RCP8.5 in the 2020s and 2080s. Between these periods and during DJF the canal bed is expected to be dry except in the 2080s under RCP8.5, when a significant amount of stream is projected in OND. Surdod exhibits the greatest increase in streamflow throughout the year, particularly in the 2080s under both RCPs up to 23%. In the 2020s, no significant increase is projected during DJF suggesting intermittent streamflow, especially under RCP2.6.

Taking the average of projected increase of precipitation under the employed RCPs in the three catchments [318 mm/y (Sana'a catchment), 397.9 mm/y (Surdod catchment), 355.2 mm/y (Siham catchment)], the distribution of rainfall in the future scenarios is as; 49% evapotranspiration, 31% runoff and outflow, 14% percolation, and 6.0% soil water. In relation to the reference period (1981–2010) as well as to the estimates indicated in previous studies (Haidera and Noaman 2010; Alhakimi 2014), the same distribution of rainfall will remain unchanged while experiencing further increase in evaporation and the surface runoff.

However, most of the few local studies (Alderwish and Al-Eryani 1999; Haidera and Noaman 2010; Alhakimi 2014), which should be acknowledged, were constrained by incomplete observational data and reliance on coarse resolution scenarios. Essential details like subbasins delineation, hydrological response units, and comprehensive soil type information are often lacking. Moreover, significant hydrological aspects such as variation in elevation, agricultural terraces that influence water quantities in the bed canal, and the control of transmission losses have been overlooked. These aspects and research gaps are fulfilled

in the current study, making it a developed work in terms of the employed data and methodology used.

Derived from the outcomes of this investigation, the consequences of climate change are not as severe as usually thought. The outcome of potential changes in future water balance components can be utilized by the local government and the local people to improve government and local strategies for water resource management and socio-economic development. The projected increase of the evapotranspiration rates driven by rising temperature warrants attention to sustain agriculture and enhance water use efficiency at the farm level. At the same time, the projected increase of the precipitation average rates offers a positive outlook for the region, allowing for increased water storage for agriculture and domestic purposes. Also, careful management can redirect floods to replenish and maintain water levels in the underground reservoirs.

In the same context, it is essential to prioritize local measures that combat and mitigate the effects of climate change. A crucial step is to strengthen local communities by implementing community-based initiatives that enhance resilience. These initiatives, for example, include training programs on sustainable agriculture, water conservation, and disaster preparedness. Future studies in Yemen will require a sufficient observational data to carry out an accurate field investigation. Additional researches could focus on acquiring accurate information to bridge the persisting data gap in the region. While this may pose challenges, alternative strategies as demonstrated in this investigation could be explored. Other downscaling techniques and application of further hydrological models are also an option for the future work in the entire Yemen.

Fostering collaboration between local communities, particularly farmers, and the government stakeholders is vital to ensure effective management of water resources and prevent conflicts over water use. This can be achieved by establishing administrative structures and institutions that support integrated water resources management (IWRM). This would require strengthening water governance mechanisms, improving data collection and monitoring systems, and facilitating stakeholder participation in decision-making processes. Moreover, implementing measures to promote infiltration and GW recharge will be crucial in the future. Actions such as constructing rain-water harvesting structures, promoting sustainable land management practices, and regulating groundwater extraction are among the most practical and effective methods to prevent depletion of the limited ground water. By prioritizing these local measures, Yemen can better adapt to the challenges of climate change, build community resilience, ensure sustainable water resource management, and safeguard against the depletion of vital groundwater sources.

Supplementary Information The online version contains supplementary material available at <https://doi.org/10.1007/s00704-024-04913-x>.

Acknowledgements We acknowledge the use of SWAT hydrological model developed by the SWAT Development Team at Texas A&M University. The author (Ali H. AL-Falahi) appreciate the scholarship of the German Academic Exchange Service (DAAD) throughout the PhD study program. Grateful thanks are extended to Professor Christian Bernhofer and Professor Matthias Mauder (Technische Universität Dresden, Institut für Hydrologie und Meteorologie – Professur für Meteorologie) for their generous financial support upon the conclusion of the scholarship, which greatly contributed to the successful completion of this work.

Author contributions All authors contributed to the study conception and design. Material preparation, data collection and analysis were performed by Ali H. AL-Falahi. Methodology and modeling guidance were performed by Ali H. AL-Falahi, Naeem Saddique, Uwe Spank, Thomas Pluntke, Solomon H. Gebrechorkos, Matthias Mauder, and Christian Bernhofer. The first draft of the manuscript was written by Ali H. AL-Falahi, reviewed and revised by Naeem Saddique, Uwe Spank, Thomas Pluntke, Solomon H. Gebrechorkos, Matthias Mauder, and Christian Bernhofer. All authors commented on previous versions of the manuscript and substantially contributed in the improvement of its content. All authors read and approved the final manuscript.

Funding Open Access funding enabled and organized by Projekt DEAL. This research did not receive any specific grant from funding agencies in the public, commercial, or not-for-profit sectors.

Data availability The data reviewed in the present study are available with the original publications and are cited at the appropriate places of the article; further inquiries can be directed to the corresponding author.

Declarations

Ethical approval We declare that this manuscript is original, has not been published before, and is not currently being considered for publication elsewhere. Further, the study has not been split up into several parts, and there is no/any violation against rights of human or institutions due to use, distribution, or publication of this work. Moreover, no conflicts of interest associated with this manuscript.

Competing interests No financial interest, but I, as a coresponding author, have to declare that the Editor-in-Chief is a co-author of this submission.

Open Access This article is licensed under a Creative Commons Attribution 4.0 International License, which permits use, sharing, adaptation, distribution and reproduction in any medium or format, as long as you give appropriate credit to the original author(s) and the source, provide a link to the Creative Commons licence, and indicate if changes were made. The images or other third party material in this article are included in the article's Creative Commons licence, unless indicated otherwise in a credit line to the material. If material is not included in the article's Creative Commons licence and your intended use is not permitted by statutory regulation or exceeds the permitted use, you will need to obtain permission directly from the copyright holder. To view a copy of this licence, visit <http://creativecommons.org/licenses/by/4.0/>.

References

- Abbasnia M, Toros H (2016) Future changes in maximum temperature using the Statistical DownScaling Model (SDSM) at selected stations of Iran. *J Model Earth Syst Environ* 2:1–7. <https://doi.org/10.1007/s40808-016-0112-z>
- Abdulla F (2020) 21st century climate change projections of precipitation and temperature in Jordan. *Proc Manuf* 44:197–204. <https://doi.org/10.1016/j.promfg.2020.02.222>
- Achamyeleh GM (2019) Techniques for calibration and validation of SWAT model in data scarce arid and semi-arid catchments in South Africa. *J Hydrol: Reg Stud* 25:100621. <https://doi.org/10.1016/j.ejrh.2019.100621>
- Al Khoury I, Boithias L, Labat D (2023) A review of the application of the Soil and Water Assessment Tool (SWAT) in karst watersheds. *Water* 15(5):954. <https://doi.org/10.3390/w15050954>
- Al Ward MA, Ismail WR (2019) Precipitation analysis and water resource of Wadi Siham Basin, Yemen. *Geografi* 7(2):36–63
- Alderwish A, Al-Eryani M (1999) An approach for assessing the vulnerability of the water resources of Yemen to climate change. *Clim Res* 12:85–89. <https://doi.org/10.3354/cr012085>
- AL-Falahi AH, Saddique N, Spank U, Gebrechorkos SH, Bernhofer C (2020) Evaluation the performance of several gridded precipitation products over the highland region of Yemen for water resources management. *Remote Sens* 12(18):2984. <https://doi.org/10.3390/rs12182984>
- Alhakimi S (2014) Water resources vulnerability and adaptation to climate change in Yemen Republic: SURDUD drainage basin. Sana'a University Publications 26:79
- Al-Jibly AA (2008) The climate change scenarios for Yemen for 2050 (Governmental Report for Environmental Protection Authority Funded by UNDP 1437). Department of Geography, Sana'a University Yemen. p 108
- Al-Mukhtar M, Qasim M (2019) Future predictions of precipitation and temperature in Iraq using the statistical downscaling model. *Arab J Geosci* 12(2):1–16. <https://doi.org/10.1007/s12517-018-4187-x>
- Alwathaf Y, El Mansouri B (2012) Hydrodynamic modeling for groundwater assessment in Sana'a Basin, Yemen. *Hydrogeol J* 20(7):1375–1392. <https://doi.org/10.1007/s10040-012-0879-6>
- Dehghan S, Salehnia N, Sayari N, Bakhtiari B (2020) Prediction of meteorological drought in arid and semi-arid regions using PDSI and SDSM: a case study in Fars Province. *Iran J Arid Land* 12(2):318–330. <https://doi.org/10.1007/s40333-020-0095-5>
- Deng C (2021) Advantages and disadvantages of terracing: A comprehensive review. *Int Soil Water Conserv Res* 9(3):344–359. <https://doi.org/10.1016/j.iswcr.2021.03.002>
- Duulatov E, Pham QB, Alamanov S, Orozbaev R, Issanova G, Asankulov T (2021) Assessing the potential of soil erosion in Kyrgyzstan based on RUSLE, integrated with remote sensing. *Environ Earth Sci* 80(18):1–13. <https://doi.org/10.1007/s12665-021-09943-6>
- EPA (2013) Yemen's second national communication under the United Nations framework convention on climate change (governmental report by the environmental protection authority in Yemen with full fund by the Global Environmental Facility (GEF) 02). EPA. p 89
- Gebrechorkos SH (2019) Impacts of projected change in climate on water balance in basins of East Africa. *Sci Total Environ* 682:160–170. <https://doi.org/10.1016/j.scitotenv.2019.05.053>
- Gebrechorkos SH, Hülsmann S, Bernhofer C (2019) Regional climate projections for impact assessment studies in East Africa. *Environ Res Lett* 14(4):044031. <https://doi.org/10.1088/1748-9326/ab055a>
- Gebrechorkos S, Bernhofer C, Hülsmann S (2020) Climate change impact assessment on the hydrology of a large river basin in Ethiopia using a local-scale climate modelling approach. *Sci Total Environ* 742:140504. <https://doi.org/10.1016/j.scitotenv.2020.140504>
- González-Rojí SJ, Wilby RL, Sáenz J, Ibarra-Berastegi G (2019) Harmonized evaluation of daily precipitation downscaled using SDSM and WRF+WRFDA models over the Iberian Peninsula. *Clim Dyn*. <https://doi.org/10.1007/s00382-019-04673-9>
- Haidera M, Alhakimi SA, Noaman A, Kebisi AA, Noaman A, Fencel A, Dougherty B, Swartz C (2011) Water scarcity and climate change adaptation for Yemen's vulnerable communities. *Local Environ* 16(5):473–488. <https://doi.org/10.1080/13549839.2011.565465>
- Haidera M, Noaman A (2010) Impact of climate change on water resources in Yemen: (case study: surdud drainage basin). In: WSTA 9th Gulf Water Conference, Sultanate of Oman
- Hashmi MZ, Shamseldin AY, Melville BW (2011) Comparison of SDSM and LARS-WG for simulation and downscaling of extreme precipitation events in a watershed. *Stoch Environ Res Risk Assess* 25:475–484. <https://doi.org/10.1007/s00477-010-0416-x>
- Hassan Z, Shamsudin S, Harun S (2014) Application of SDSM and LARS-WG for simulating and downscaling of rainfall and temperature. *Theor Appl Climatol* 116:243–257. <https://doi.org/10.1007/s00704-013-0951-8>
- Homsy R, Shiru MS, Shahid S, Ismail T, Harun SB, Al-Ansari N, Chau K-W, Yaseen ZM (2020) Precipitation projection using a CMIP5 GCM ensemble model: a regional investigation of Syria. *Eng Appl Comput Fluid Mech* 14(1):90–106. <https://doi.org/10.1080/19942060.2019.1683076>
- IPCC (2022) Climate change 2022: impacts, adaptation and vulnerability. Contribution of working group II to the sixth assessment report of the intergovernmental panel on climate change (intergovernmental panel on climate change 6; p. 3056). <https://doi.org/10.1017/9781009325844>
- Jafari H (2019) Contribution of rainfall and agricultural returns to groundwater recharge in arid areas. *J Hydrol* 575:1230–1238. <https://doi.org/10.1016/j.jhydrol.2019.06.029>
- Janjić J, Tadić L (2023) Fields of application of SWAT hydrological model—a review. *Earth* 4(2):331–344. <https://doi.org/10.3390/earth4020018>
- Khelifa WB, Hermassi T, Strohmeier S, Zucca C, Ziadat F, Boufaroua M, Habaieb H (2017) Parameterization of the effect of bench terraces on runoff and sediment yield by SWAT modeling in a small semi-arid watershed in Northern Tunisia. *Land Degrad Dev* 28(5):1568–1578. <https://doi.org/10.1002/ldr.2685>
- Klaas DKSY, Imteaz MA, Sudiayem I, Klaas EME, Klaas ECM (2018) Simulating future climate projection under HadCM3 GCM scenarios on a tropical karst island using SDSM: A case study of tropical karst catchment in Rote Island, Indonesia. *IOP Conf Ser: Earth Environ Sci* 200:012018. <https://doi.org/10.1088/1755-1315/200/1/012018>
- Koltsida E, Mamassis N, Kallioras A (2023) Hydrological modeling using the Soil and Water Assessment Tool in urban and peri-urban environments: the case of Kifisos experimental subbasin (Athens, Greece). *Hydrol Earth Syst Sci* 27(4):917–931. <https://doi.org/10.5194/hess-27-917-2023>
- Kumar N, Singh SK, Srivastava PK, Narsimlu B (2017) SWAT model calibration and uncertainty analysis for streamflow prediction of the Tons River Basin, India, using Sequential Uncertainty Fitting (SUFI-2) algorithm. *Model Earth Syst Environ* 3(1):1–13. <https://doi.org/10.1007/s40808-017-0306-z>
- Lotfi M, Kamali GA, Meshkatee AH, Varshavian V (2022) Performance analysis of LARS-WG and SDSM downscaling models in simulating temperature and precipitation changes in the West of Iran. *Model Earth Syst Environ* 8(4):4649–4659. <https://doi.org/10.1007/s40808-022-01393-8>
- Magombeyi MS, Taigbenu AE, Barron J (2018) Effectiveness of agricultural water management technologies on rainfed cereals crop yield and runoff in semi-arid catchment: a meta-analysis. *Int J*

- Agric Sustain 16(4):418–441. <https://doi.org/10.1080/14735903.2018.1523828>
- Mapes KL, Pricope NG (2020) Evaluating SWAT model performance for runoff, percolation, and sediment loss estimation in low-gradient watersheds of the Atlantic coastal plain. *Hydrology* 7(2):21. <https://doi.org/10.3390/hydrology7020021>
- Masoud MHZ, Basahi JM, Zaidi FK (2018) Assessment of artificial groundwater recharge potential through estimation of permeability values from infiltration and aquifer tests in unconsolidated alluvial formations in coastal areas. *Environ Monit Assess* 191(1):31. <https://doi.org/10.1007/s10661-018-7173-6>
- Melki A (2017) Groundwater recharge estimation under semi-arid climate: case of Northern Gafsa watershed, Tunisia. *J Afr Earth Sc* 132:37–46. <https://doi.org/10.1016/j.jafrearsci.2017.04.020>
- Moriassi DN (2015) Hydrologic and water quality models: performance measures and evaluation criteria. https://www.researchgate.net/publication/289540757_Hydrologic_and_Water_Quality_Models_Performance_Measures_and_Evaluation_Criteria. Accessed 10.01.2023
- Nasiri S, Ansari H, Ziaei AN (2020) Simulation of water balance equation components using SWAT model in Samalqan Watershed (Iran). *Arab J Geosci* 13(11):1–15. <https://doi.org/10.1007/s12517-020-05366-y>
- Ouessar M, Bruggeman A, Abdelli F, Mohtar RH, Gabriels D, Cornelis WM (2009) Modelling water-harvesting systems in the arid south of Tunisia using SWAT. *Hydrol Earth Syst Sci* 13(10):2003–2021. <https://doi.org/10.5194/hess-13-2003-2009>
- Pani A, Ghatak I, Mishra P (2021) Understanding the water conservation and management in India: an integrated study. *Sustain Water Resour Manag* 7(5):77. <https://doi.org/10.1007/s40899-021-00556-2>
- Saddique N, Usman M, Bernhofer C (2019a) Simulating the impact of climate change on the hydrological regimes of a sparsely gauged mountainous basin, Northern Pakistan. *Water* 11(10):2141. <https://doi.org/10.3390/w11102141>
- Saddique N, Usman M, Bernhofer C, Kronenberg R (2019b) Downscaling of CMIP5 models output by using statistical models in a data scarce mountain environment (Mangla Dam Watershed), Northern Pakistan. *Asia-Pac J Atmos Sci* 55. <https://doi.org/10.1007/s13143-019-00111-2>
- Tahir T, Hashim A, Wan Yusof K (2018) Statistical downscaling of rainfall under transitional climate in Limbang River Basin by using SDSM. *IOP Conf Ser: Earth Environ Sci* 140:012037. <https://doi.org/10.1088/1755-1315/140/1/012037>
- Tukimat NNA, Ahmad Syukri NA, Malek MA (2019) Projection the long-term ungauged rainfall using integrated Statistical Downscaling Model and Geographic Information System (SDSM-GIS) model. *Heliyon* 5(9):e02456. <https://doi.org/10.1016/j.heliyon.2019.e02456>
- Van der Gun J, Ahmed A (1995) The water resources of Yemen: a summary and digest of available information; technical report. Ministry of Oil and Mineral Resources: Sanaa, Yemen, 1995. [Google Scholar]
- Varisco D (2019) Pumping Yemen dry: a history of Yemen's water crisis. *Hum Ecol* 47. <https://doi.org/10.1007/s10745-019-0070-y>
- Wang Y (2021) Grassland soil moisture fluctuation and its relationship with evapotranspiration. *Ecol Ind* 131:108196. <https://doi.org/10.1016/j.ecolind.2021.108196>
- Weiss MI (2015) A perfect storm: the causes and consequences of severe water scarcity, institutional breakdown and conflict in Yemen. *Water Int* 40(2):251–272. <https://doi.org/10.1080/02508060.2015.1004898>
- Worku G, Teferi E, Bantider A, Dile YT (2020) Prioritization of watershed management scenarios under climate change in the Jemma sub-basin of the Upper Blue Nile Basin, Ethiopia. *J Hydrol: Reg Stud* 31:100714. <https://doi.org/10.1016/j.ejrh.2020.100714>
- Zhang D, Lin Q, Chen X, Chai T (2019) Improved Curve Number Estimation in SWAT by Reflecting the Effect of Rainfall Intensity on Runoff Generation. *Water* 11(1):163. <https://doi.org/10.3390/w11010163>

Publisher's Note Springer Nature remains neutral with regard to jurisdictional claims in published maps and institutional affiliations.